Inverse synchronization in semiconductor laser diodes

S. Sivaprakasam, Iestyn Pierce,* Paul Rees, Paul S. Spencer, and K. Alan Shore
School of Informatics, University of Wales, Bangor, Dean Street, Bangor, Gwynedd LL57 1UT, United Kingdom

Angel Valle
Instituto de Física de Cantabria and Consejo Superior de Investigaciones Cientificas, Universidad de Cantabria, Avenida de Los Castros s/n, 39005 Santander, Spain

(Received 18 October 2000; published 31 May 2001)

The study of nonlinear dynamical systems is a subject of much interest, one application being in secure communication systems realized through the synchronization of chaotic dynamical systems. In this paper optical coupling is used to effect synchronization between two diode lasers in a master-slave configuration, and we study the effect of frequency detuning between the master and slave lasers on the character of the observed synchronization. Experimental conditions are found under which the synchronization plot (formed by plotting the output power of the slave laser against that of the master at each instant in time) makes a transition from a positive gradient to a negative gradient. The appearance of such a negative gradient is a new phenomenon, to our knowledge, which we term ''inverse synchronization.'' A rate-equation model is proposed which accounts for light injection into the slave laser, and which agrees with the experimental results. Using this model, we etablish that inverse synchronization is caused by nonresonant coupling between the master and slave lasers.

DOI: 10.1103/PhysRevA.64.013805 PACS number(s): 42.65.Sf

I. INTRODUCTION

Synchronization of chaotic systems has been given much attention due to its potential in secure communication systems. The underlying concept is that the transmitted message should be encoded within the noiselike output of a chaotic transmitter. Extraction of the message requires a receiver in which the same chaos is generated as in the transmitter, which can be achieved by synchronization of the chaos [1] of the transmitter and the receiver. A successful demonstration of chaotic transmission of a message using a fiber laser [2] was reported recently. Progress has been made toward experimental encryption and decryption by use of an interesting form of wavelength chaos [3]. Because of the ease of operation of semiconductor lasers, previous work [4] aimed to develop a chaotic communication system utilizing these lasers as the source of optical chaos. Encoding and effective decoding of a message depend critically on the quality of synchronization between the two chaotic lasers used as transmitter and receiver. Hence synchronization, and its dependence on various experimental parameters, are of paramount importance. The most common method of characterizing the quality of synchronization of two lasers is to plot a synchronization diagram: at each point in time the intensity of one laser is plotted as a function of the intensity of the other. If the two lasers are perfectly synchronized, the synchronization plot will be a straight line with a positive gradient. Less than perfect synchronization leads to a broadening of the plot.

In this paper we study the synchronization of a laser diode to an external optical signal generated by another laser diode which is subjected to optical feedback. The systems being synchronized are therefore nonidentical. When the fundamental emission frequency of one of the lasers is varied, a detuning is effected between the two lasers. Varying the detuning leads to changes in the character of the synchronization. We report what we believe to be the first experimental observation of a transition in the synchronization plot from a positive gradient to a negative gradient [5]. We term this negative gradient phenomenon ''inverse synchronization.'' For a zero detuning between the transmitter and receiver the resulting synchronization diagram has a positive gradient. For sufficiently large detuning the system operates in the inverse synchronization regime, with a negative gradient in the synchronization diagram.

The phenomenon of inverse synchronization has been observed experimentally when the master laser exhibits both stable and unstable chaotic dynamics. Chaotic operation of the master laser is induced through external optical feedback [6]. We report experimental synchronization diagrams for chaotic operation for a number of detunings. Experimental synchronization diagrams are also displayed for operation in the low-frequency fluctuation (LFF) regime. This regime of operation has the advantage over the fully chaotic case of more clearly illustrating the inverse behavior in the time domain. A model is presented that explains the in-phase and antiphase behaviors seen for different frequency detunings by accounting for both resonant and nonresonant coupling between the master and slave lasers. The model is first demonstrated for the simple case of sinusoidally varying injection from the master laser to the slave laser. The model shows excellent agreement with measurements undertaken for sinusoidal injection. The model is also seen to give excellent qualitative agreement with measurements when it is applied to the cases of chaotic and LFF operation.

II. EXPERIMENT

The experimental arrangement used to make the measurements described in this work is shown schematically in Fig.

*Email address: iestyn@informatics.bangor.ac.uk

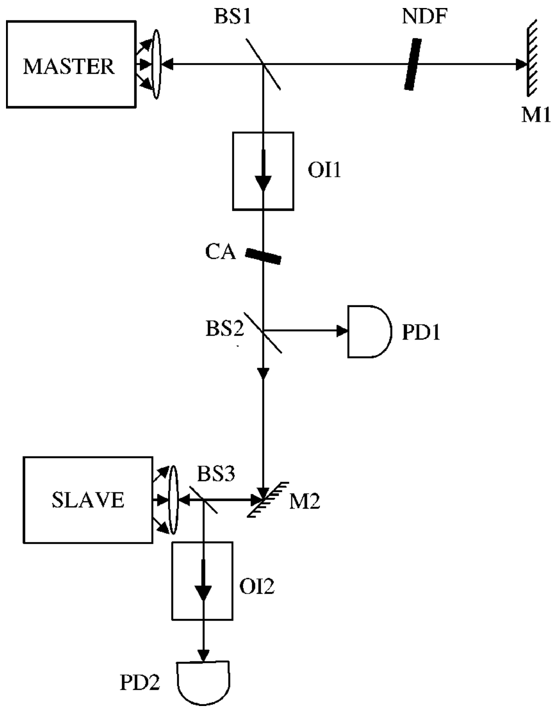

FIG. 1. Experimental setup: BS1–BS3: beam splitters; NDF: neutral density filter; M1 and M2: mirrors; PD1 and PD2: photodetectors; CA: coupling attenuator; OI1 and OI2: optical isolators.

1. We have used two single mode Fabry-Perot diode lasers emitting at a wavelength of 830 nm, with a linewidth of 200 MHz for our experiments. These lasers are driven by ultralow noise current sources (ILX-Lightwave, LDX 3620) with a current noise spectral density of 1 pA/$\sqrt{\text{Hz}}$. These lasers are temperature controlled by thermoelectric controllers (ILX-Lightwave, LDT 5412) to a precision of 0.01 K. The master laser is subjected to optical feedback from an external mirror (M1), and the feedback strength is controlled using a continuously variable neutral density filter (NDF). The cavity length is fixed at 80 cm throughout the experiment. The optical isolators ensure that the lasers experience minimal back reflection, with typical isolation of -41 dB. An isolator (OI1) ensures that the master laser is isolated from the slave laser. The coupling attenuator (CA) enables control of the percentage of master power fed into the slave laser. The two idential photodetectors (PD1) and (PD2) (New Focus, 1621) have response times of 2 ns. The output of the master laser is coupled to photodetector (PD1) by the beam splitters (BS1) and (BS2). The output of the master laser is coupled to the slave laser via mirror (M2). Beam splitter (BS3) couples the slave laser output to photodetector (PD2). The photodetector outputs are stored in a digital storage oscilloscope (LeCroy, LC564A) and then acquired by a personal computer.

Detuning is effected between the two lasers by varying the bias current of the slave laser. At the operating point chosen for the experimental results presented, a change in the bias current of the laser of 1 mA shifts the laser emission by 1 GHz, and this is used as a scaling factor to calculate the detuning for all other bias points. It is noted that if the master laser is subjected to sufficient optical feedback to drive its output chaotic, its linewidth is greatly broadened. In this case the detuning is defined as the difference between the peak emission frequencies of the solitary lasers. At a fixed value of the detuning, the slave laser intensity output is plotted against the master laser intensity output in order to obtain a synchronization plot. Throughout this paper the detuning will be defined as the frequency of the light injected from the master laser (and denoted ω_{inj}) minus the frequency of the slave laser mode (denoted ω_{mode}). The detuning $\Delta\omega$ is therefore defined as

$$\Delta\omega = \omega_{inj} - \omega_{mode}. \tag{1}$$

Synchronization plots for four different values of detuning are shown in Fig. 2, where the external optical feedback into the master laser has been adjusted such that the master laser output exhibits a chaotic variation in amplitude. Earlier theoretical studies showed that synchronization is best achieved when the detuning between the two diode lasers is zero [7]. A positive or negative detuning arises depending on the value of the slave bias current. A typical synchronization plot is shown in Fig. 2(b), where the gradient of the synchronization plot is positive, corresponding to zero detuning between master and slave lasers.

Figure 2(a) shows a degradation in synchronization for a positive detuning of $+6$ GHz. In this case there is no correlation between the intensities of the master and slave lasers. This lack of correlation for positive detuning will be discussed in relation to our model in Sec. III.

As the detuning is made negative, the synchronization plot starts to branch with a portion of negative gradient as shown in Fig. 2(c) for a detuning of -3 GHz. As the detuning is further increased to -6 GHz, the newly developed branch with a negative gradient dominates and the branch with a positive gradient disappears. This is shown in Fig. 2(d). To the authors' knowledge the appearance of a negative gradient in the synchronization diagram of two coupled lasers is a new observation, and it is termed ''inverse synchronization.'' In order to verify that the detuning between master and slave lasers is the only factor which determines the regime of operation, detuning was also effected by varying the operating temperatures of the both master and slave lasers, and the same phenomena were reproduced.

The effect of different regimes of chaotic operation on the results presented in Fig. 2 is examined by repeating the measurements with the master laser operating conditions varied to yield low-frequency fluctuations in the master laser output [8], observed when the laser is biased near threshold and is subjected to moderate external optical feedback. Figure 3 shows very similar behavior to the chaotic case shown in Fig. 2. In particular, the system is seen to yield conventional, positive slope synchronization for small detuning [Fig. 3(b)] and inverse synchronization when the detuning is larger [Fig. 3(d)].

The time-domain measurements illustrated in Fig. 4 show the dropouts in power that are characteristic of LFF's. These dropouts serve as direct time-domain evidence of the antiphase behavior seen in the synchronization diagrams for large detunings. Having described observations of inverse

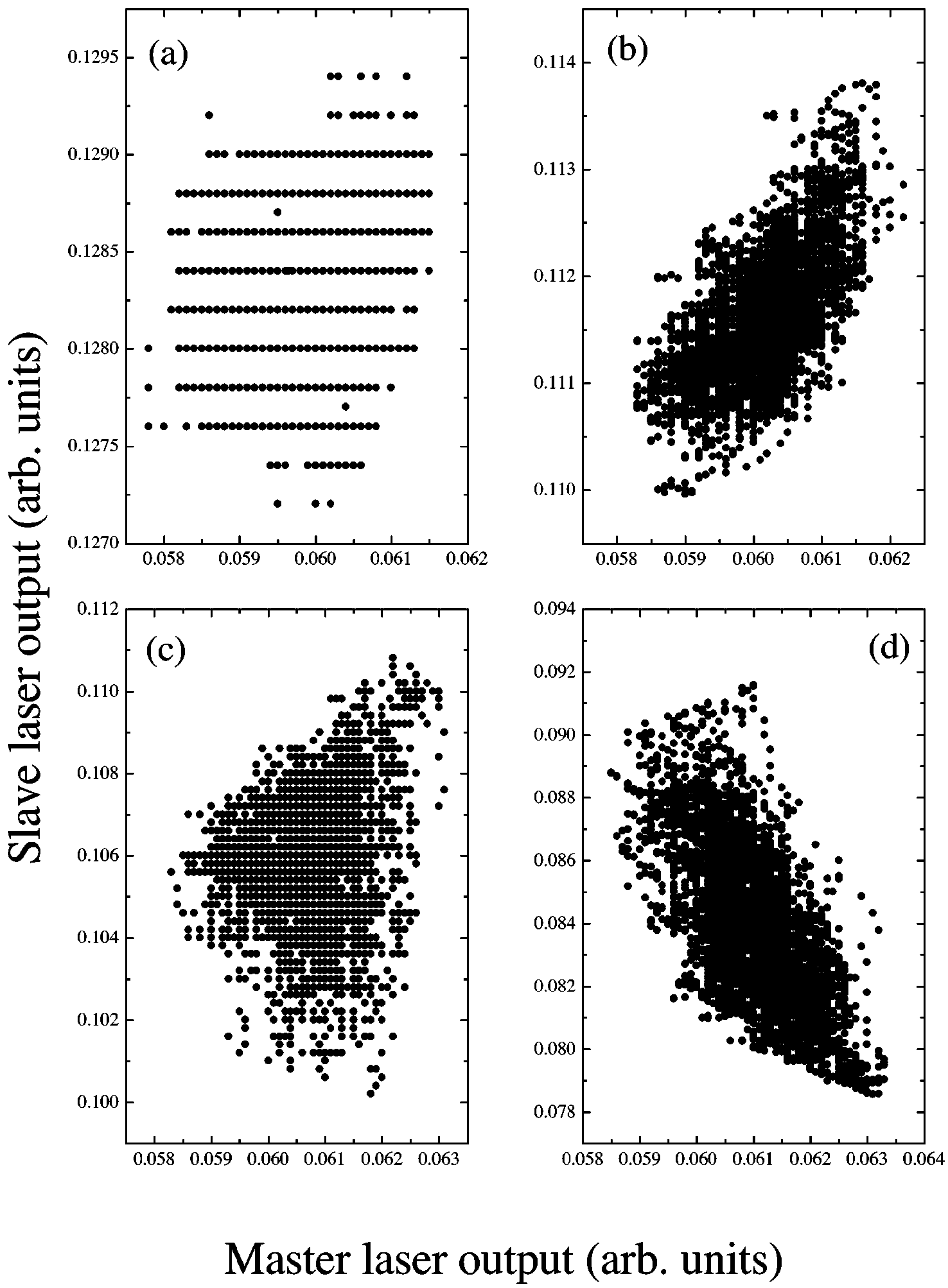

FIG. 2. Measured synchronization plots for master-slave detunings of (a) $+6$ GHz, (b) 0 GHz, (c) -3 GHz, and (d) -6 GHz, and chaotic master laser output.

synchronization behavior for a range of detunings in a master-slave configuration, Sec. III proposes a model to explain this behavior based on resonant and nonresonant coupling between the two lasers.

III. MODEL

As suggested in Sec. II, the model must account for ‘‘normal’’ (positive gradient) synchronization when the detuning between master and slave lasers is small, and must also reproduce the negative gradient (inverse synchronization) behavior when the detuning is larger. Because positive gradient behavior occurs when the detuning is small, it follows that such a behavior is a resonant effect: the light injected from the master laser overlaps in wavelength to a large degree with the slave laser mode. If the injected light increases in intensity, this leads to an increased injection into the slave laser mode, which increases the intensity of the slave laser output. This leads to an in-phase behavior, and the corresponding synchronization diagram has a positive gradient.

If the injected light is detuned from the slave laser mode wavelength then there is very little coupling into the slave lasing mode. In this operating regime the dominant effect is nonresonant amplification. Even though it is not resonant with the slave laser mode, the light coupled in from the master laser is still amplified through the stimulated emission process. Furthermore, since the injected light does not meet the laser round-trip phase condition [9] it is a good approximation to assume that the amplified light only makes a single pass through the device before being lost from the laser cavity. The effect of this nonresonant amplification of light that does not couple into the slave laser mode is a reduction in

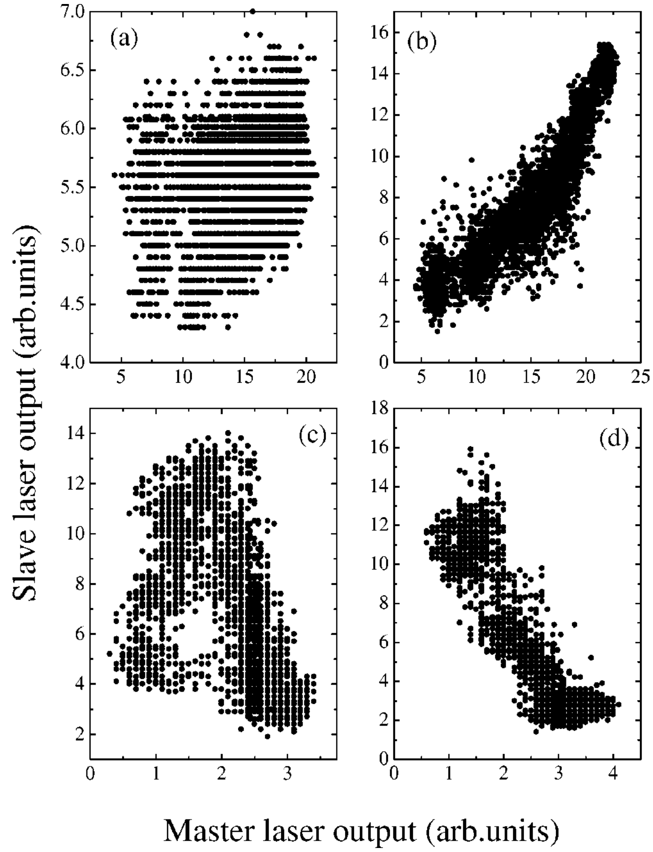

FIG. 3. Measured synchronization plots for master-slave detuning of (a) $+6$ GHz, (b) 0 GHz, (c) -3 GHz, and (d) -6 GHz, and with the master laser operating in a low-frequency fluctuation regime.

the carrier density in the device, since each stimulated emission event leads to the loss of one electron-hole pair. If the intensity of the injected light is increased, then the rate at which the nonresonant amplification process removes carriers from the reservoir is also increased. This leaves fewer carriers to take part in the gain process for the slave laser mode, reducing the optical output. Nonresonant amplification therefore leads to antiphase behavior between the intensities of the master and slave laser outputs.

The qualitative arguments of the previous paragraphs are made more concrete by including the effects of resonant and nonresonant coupling in a standard rate-equation model for a slave laser with a quantum-well gain region. The rate equation for the carrier density N in the slave laser is given by

$$\frac{dN}{dt}=\frac{J_{inj}}{wq}-\frac{J_{spon}}{wq}-\frac{N}{\tau_c}-g(\omega_{mode})Sv_g -[\kappa_{nr}\exp\{g(\omega_{inj})L\}S_{inj}], \tag{2}$$

where J_{inj} is the injection current density, J_{spon} is the effective spontaneous emission current (obtained from a first-principles optical gain calculation), q is the electronic charge, w is the quantum-well width, τ_c is the carrier lifetime in the semiconductor medium, $g(\omega)$ is the optical gain, v_g is the group velocity of the optical mode, L is the laser cavity length, S is the photon density in the slave laser mode, S_{inj} is the injected photon density, and κ_{nr} accounts for the nonresonant coupling of the injected light into the slave laser. The injected light is assumed to be centered about the optical circular frequency ω_{inj}, while the slave laser mode frequency is ω_{mode}.

The first two terms in Eq. (2) describe an electrical pumping of the carrier reservoir and carrier loss through spontaneous emission, while the third term accounts for carrier loss through nonradiative recombination. The fourth term accounts for carrier loss due to amplification of the photons in the slave laser mode. These first four terms are the same as the terms in a standard semiconductor laser model. This standard carrier rate equation is augmented by the addition of a

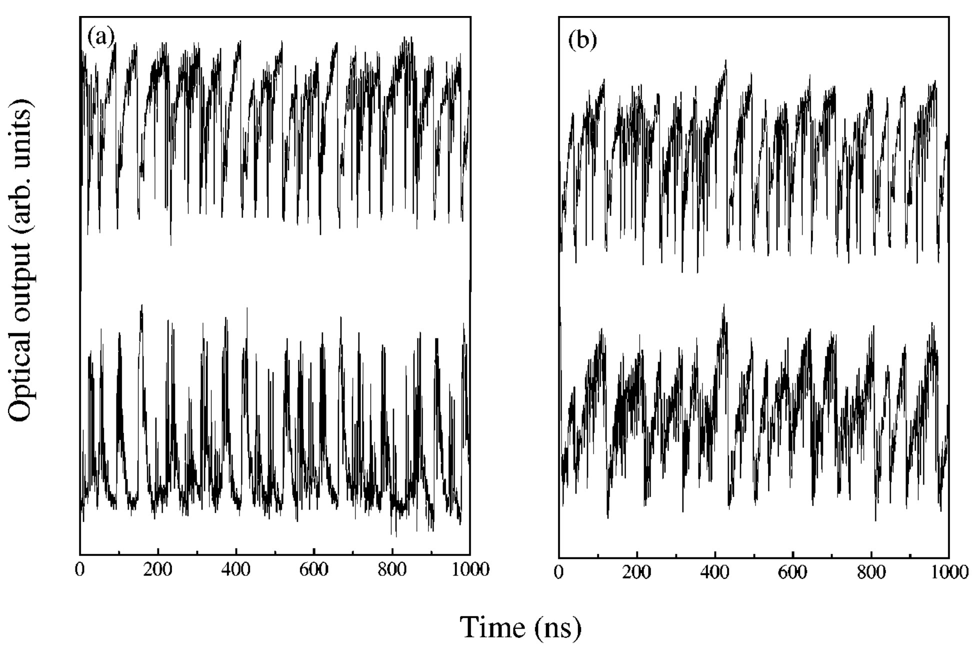

FIG. 4. Measured time traces of the master (upper traces) and slave (lower traces) lasers for detunings (a) -6 GHz and (b) 0 GHz and with the master laser operating in the low-frequency fluctuation regime.

fifth term (in square brackets) which accounts for carriers lost through single-pass amplification of the injected light at frequency ω_{inj}.

The standard semiconductor laser rate equation for the photon density is modified in a similar way,

$$\frac{dS}{dT}=\Gamma g(\omega_{mode})Sv_g-\frac{S}{\tau_p}+\beta\frac{J_{spon}}{wq}+[\kappa_{res}S_{inj}], \quad (3)$$

where Γ is the confinement factor of the optical mode with the quantum-well gain region, τ_p is the photon lifetime, β is the spontaneous emission coupling factor, and κ_{res} accounts for resonant coupling of the injected light into the slave laser mode.

The first three terms account for the increase in the photon density due to amplification of the slave laser mode, losses from the laser facets and from scattering processes, and spontaneous emission. The fourth term (again in square brackets) is in addition to the standard rate-equation terms, and accounts for the coupling of the injected light into the slave laser mode.

With the modifications to a standard laser rate-equation model detailed by the terms in square brackets in Eqs. (2) and (3) the phenomena of normal, positive slope, synchronization and inverse synchronization occur depending on the relative dominance of the two extra terms, dictated by the coupling strengths κ_{nr} and κ_{res}, which are related, as will be described in Sec. IV.

IV. RESULTS AND DISCUSSION

So far in the analysis presented in this paper, no assumptions have been made about the dynamics of the injected light. In Sec. II experimental results were shown for the cases when the master laser operated in the fully chaotic and low-frequency fluctuation regimes. In both cases the behavior of the slave laser was dictated by the detuning between the master and slave lasers. This leads us to believe that the inverse synchronization phenomenon does not depend on the master laser being in any particular chaotic state. Operation in the LFF or chaotic regimes has the notable disadvantage that the line shape, and consequently the spectral overlap between the injected light and the slave laser mode, is difficult to quantify. In order to describe the mechanism for inverse synchronization more clearly, it is advantageous to examine the simpler case when the variation in master laser intensity is not chaotic at all: the case of sinusoidal intensity variation. This has the benefit over the chaotic case of the line shape being well approximated by a Lorentzian function.

By assuming that the master and slave lasers have a Lorentzian line shape, and taking the overlap integral of the two line shapes, it is possible to calculate a value for the resonant coupling rate, κ_{res},

$$\kappa_{res}=\frac{K_1}{1+\left(\frac{\Delta\omega}{2\pi\Delta\nu}\right)^2}, \quad (4)$$

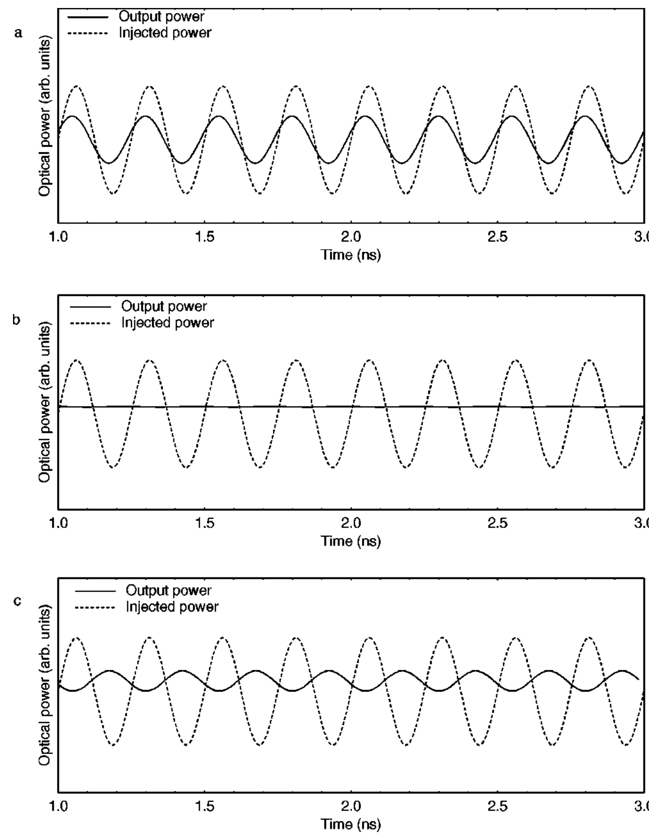

FIG. 5. Simulated variation of master and slave laser intensities for detunings of (a) 0 GHz, (b) -4 GHz, and (c) -8 GHz with a sinusoidally varying injection intensity.

where $\Delta\nu$ is the continuous-wave linewidth of the modes (assigned the experimentally determined value 200 MHz in this analysis), $\Delta\omega$ is the detuning defined in Eq. (1), and K_1 accounts for the extrinsic coupling loss. The nonresonant coupling rate κ_{nr} is related to the resonant coupling rate κ_{res} by the relation

$$\kappa_{nr}=K_2\left[1-\frac{\kappa_{res}}{K_1}\right], \quad (5)$$

where K_2 accounts for the extrinsic losses for nonresonant coupling.

Figure 5 shows the result of numerical solution of Eqs. (2) and (3) for zero detuning and for large (-8 GHz) detuning when the injected light exhibits a sinusoidal variation. For the case of zero detuning the coupling rate κ_{res} has its maximum value. In this case the variation in the intensity of the slave laser output is seen to be in phase with the injected light. This is as expected, because the resonant coupling term in the photon equation dominates. The extra coupling term in Eq. (3) accounts for this normal, positive slope synchronization behavior, since an increase in the injected light intensity, S_{inj}, leads to an increase in the slave laser mode intensity S whose magnitude is dictated by the coupling rate κ_{res}.

When the detuning is changed to -8 GHz, the resonant coupling becomes negligible, and the term in κ_{nr} is seen to dominate. In this case, illustrated in Fig. 5(c), an increase in the injected light intensity leads to a reduction in the carrier density which in turn reduces the output of the slave laser mode. This is the inverse synchronization regime for sinusoidal excitation. The extra term in Eq. (2) accounts for this negative slope inverse synchronization behavior. If the coupling κ_{nr} is the dominant term, then the system operates with the variation in the slave laser intensity in antiphase with the injected light. Conversely, if the term with coupling strength κ_{res} is dominant, then the slave laser intensity varies in phase with the injected light.

For an intermediate detuning of -4 GHz [shown in Fig. 5(b)], the amplitude of the output wave form is seen to be much reduced, since the opposing effects of resonant and nonresonant amplification almost cancel. At such intermediate detunings in a practical system, noise would dominate the behavior, and neither conventional nor inverse synchronization would be discernible. In order to concentrate on the mechanism of inverse synchronization, noise is not included in this work, since its only effect would be a trivial broadening of the synchronization diagrams and time traces.

Due to the symmetry of the variation in the coupling strengths with detuning [decribed by Eq. (4)] for positive and negative detunings, our model also predicts that inverse synchronization should occur for large positive detunings, in contradiction of the experimental results presented in Fig. 2(a). In order to address this apparent anomaly, we replaced the photon density in our model with a complex electric field, thereby including the effect of phase-amplitude coupling, known to cause asymmetry in behavior with detuning in continuous-wave injection-locking studies [10]. The resulting complex electric-field model yielded results identical to the photon-density model, with inverse synchronization predicted for large detunings of either sign. The observed asymmetry with detuning is therefore due to some other effect, possibly power variation. Because the slave laser is tuned by changing its drive current or operating temperature, its output power is also changed. For the case of positive detuning the slave laser output power is increased; therefore, the master laser power coupled into the slave laser is reduced in proportion to the zero detuning case. For positive detunings we conjecture that more injected power than is available in our experimental setup would be required to effect inverse synchronization. The variation of the quality of synchronization with slave laser power will be the subject of further work. For the work presented in this paper, we will therefore limit consideration to zero and negative detunings. We further choose to retain the photon-density model, since it emphasizes that the nonresonant coupling mechanism for inverse synchronization is an incoherent effect.

We now verify our model by confirming experimentally that both positive gradient synchronization and inverse synchronization can take place for sinusoidally modulated injected light by varying the detuning between master and slave. By eliminating the optical feedback into the master laser in Fig. 1, so that the laser operates in a stable regime, and adding a sinusoidal modulation to the drive current, the results illustrated in Fig. 6 were obtained experimentally. Again, in this case for small detuning, the slave laser output varies in phase with the injected light [as shown in Fig. 6(a)],

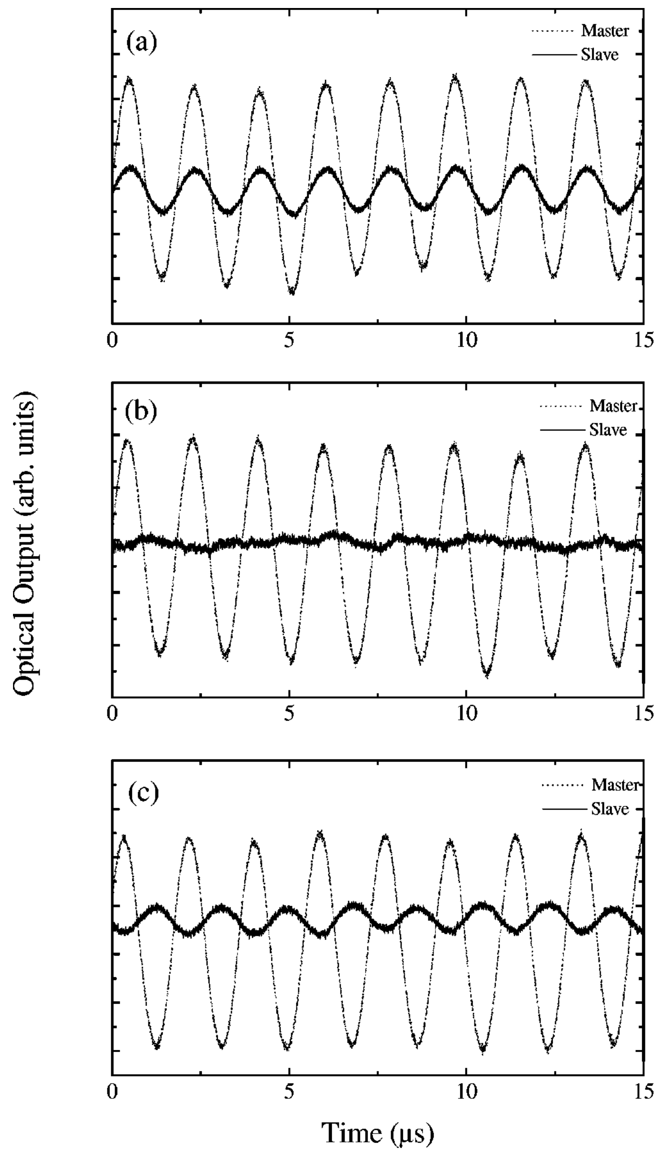

FIG. 6. Measured variation of master and slave laser intensities for detunings of (a) 0 GHz, (b) -4 GHz, and (c) -8 GHz with a sinusoidally varying injection intensity.

which is behavior identical to that predicted by the model in Fig. 5(a). For large detuning [shown in Fig. 6(c)] the slave laser exhibits inverse synchronization, with the input and output intensities in antiphase, again in close agreement with the prediction of the model shown in Fig. 5(c). This experimental evidence of inverse synchronization behavior for sinusoidally varying injection reinforces the argument that the relative dominance of resonant and nonresonant amplification dictates the regime of operation.

Figure 6 also shows the experimentally obtained output for intermediate detuning. In this case the two effects of resonant and nonresonant amplification are almost equal in their influence, and it is very difficult to discern either an in-phase or antiphase relationship between the injected light and the slave laser output: without the dominance of either effect, the variation in slave laser output is seen to be controlled by noise. The fact that the crossover between inverse

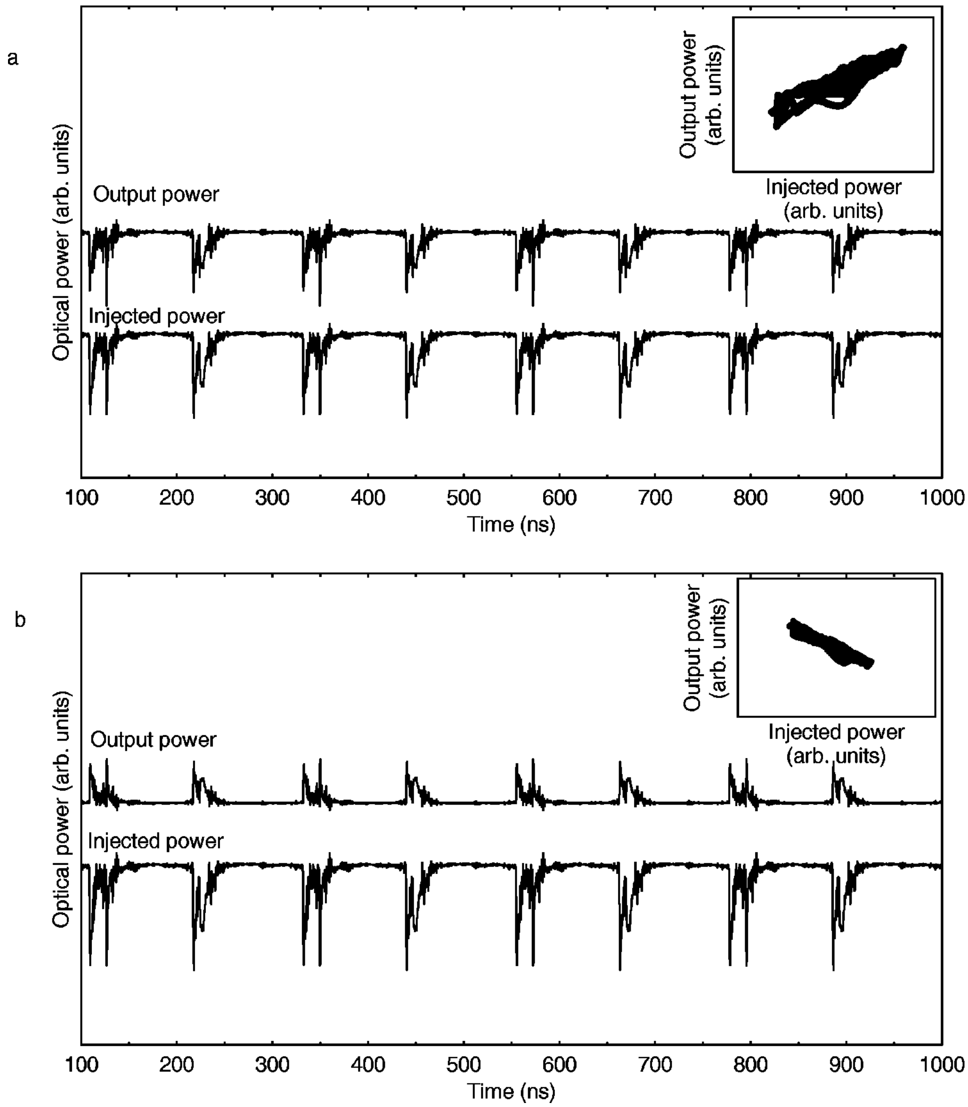

FIG. 7. Simulated variation of master and slave laser intensities for detunings of (a) 0 GHz and (b) -8 GHz, with the master laser operating in the low-frequency fluctuation regime. Insets show synchronization plots.

synchronization and positive-slope synchronization occurs at a detuning of -4 GHz, in agreement with the model, is somewhat fortuitous, since the crossover is dictated by the experimentally determined laser linewidth $\Delta\nu$ and the phenomenological coupling constants K_1 and K_2. In fact inverse synchronization behavior does not depend critically on the values of K_1 and K_2.

Although the assumption of Lorentzian line shape employed in the case of sinusoidal modulation is not such a good approximation for chaotic operation, we obtain further qualitative verification of our model by comparing results from the model with experiment when the master laser is operated in the LFF regime. In order to reproduce the experimental results for the case of LFF input, the model described by Eqs. (2) and (3) was driven by the output of a Lang-Kobayashi model of a laser diode with optical feedback [11] operating in the LFF regime. Figure 7 shows time traces and synchronization plots for zero detuning and for a detuning of -8 GHz. For both cases the behavior shows the same trends as for the sinusoidal case. When the detuning is small the injected light couples into the slave laser mode and the output light and injected light are in phase, as can clearly be seen with reference to the dropouts in the time domain traces. When the detuning is increased to -8 GHz, very little of the injected light couples into the slave laser mode, and the dominant effect is once again nonresonant amplification of the injected light which changes the carrier density in the slave laser and leads to a negative slope in the synchronization diagram.

V. CONCLUSIONS

In conclusion we have studied the effect of detuning on the character of synchronization of two semiconductor laser diodes in a master-slave configuration where the master laser is operated in several dynamical regimes controlled by external optical feedback. We report the observation of synchronization with a negative gradient between two lasers for large detunings, a phenomenon which we have termed inverse synchronization. The character of the synchronization is seen to be controlled by the degree of detuning between the master and slave lasers.

The observation of both conventional, positive gradient synchronization and inverse synchronization was explained using a rate-equation model of the slave laser which incorporated the effects of resonant and nonresonant amplification of the light injected from the master laser. The results of the rate-equation model reproduce the measurements presented in this paper. When resonant amplification is the dominant effect, the synchronization is seen to have a positive slope, but when nonresonant amplification dominates there is inverse synchronization between master and slave lasers. Varying the temperatures of the laser diodes confirms that the changeover between conventional and inverse synchronization is caused by a detuning between the master and slave lasers. Since the antiphase relationship between the master and slave lasers is preserved not only for chaotic regimes of operation but also for nonchaotic regimes such as sinusoidal power variation, we suggest that varying the detuning between two coupled lasers should prove useful for phase inversion in optical signal processing applications.

ACKNOWLEDGMENTS

The work was supported by UK-EPSRC Grant No. GR/K78799. Discussions with Yanhua Hong are gratefully acknowledged.

[1] L.M. Pecora and T.L. Carroll, Phys. Rev. Lett. **64**, 821 (1990); T. Sugawara, M. Tachikawa, T. Tsukamoto, and T. Shimizu, *ibid.* **72**, 3502 (1994); R. Roy and K.S. Thornburg, Jr., *ibid.* **72**, 2009 (1994).

[2] G.D. VanWiggeren and R. Roy, Science **279**, 1198 (1998); Phys. Rev. Lett. **81**, 3547 (1998).

[3] L. Larger, J.P. Goedgebuer, and F. Delorme, Phys. Rev. E **57**, 6618 (1998).

[4] S. Sivaprakasam and K.A. Shore, Opt. Lett. **24**, 466 (1999); **24**, 1200 (1999); IEEE J. Quantum Electron. **QE-36**, 35 (2000).

[5] S. Sivaprakasam and K. A. Shore, in IEEE/OSA Conference on Lasers and Electro-Optics, San Francisco, 2000 (unpublished).

[6] K. Petermann, *Laser Diode Modulation and Noise* (Kluwer, Boston, 1988).

[7] P.S. Spencer and C.R. Mirasso, IEEE J. Quantum Electron. **QE-35**, 803 (1999); P.S. Spencer, C.R. Mirasso, P. Colet, and K.A. Shore, *ibid.* **QE-34**, 1673 (1998).

[8] J. Sacher, W. Elsasser, and E.O. Gobel, Phys. Rev. Lett. **63**, 2224 (1989); G.H.M. vanTartwijk, A.M. Levine, and D. Lenstra, IEEE J. Sel. Top. Quantum Electron. **1**, 466 (1995); T. Sano, Phys. Rev. A **50**, 2719 (1994); I. Fischer, G.H.M. van-Tartwijk, A.M. Levine, W. Elsasser, E. Gobel, and D. Lenstra, Phys. Rev. Lett. **76**, 220 (1996); Y. Takiguchi, Y. Lui, and J. Ohtsubo, Opt. Lett. **23**, 1369 (1998).

[9] L.A. Coldren and S.W. Corzine, *Diode Lasers and Photonic Integrated Circuits* (Wiley, New York, 1995).

[10] F. Mogensen, H. Olesen, and G. Jacobsen, IEEE J. Quantum Electron. **QE-21**, 784 (1985); I. Petitbon, P. Gallion, G. Debarge, and C. Chabran, *ibid.* **QE-24**, 148 (1998).

[11] R. Lang and K. Kobayashi, IEEE J. Quantum Electron. **QE-16**, 347 (1980).